Journal of Environmental Chemical Engineering 10 (2022) 107277

Contents lists available at ScienceDirect

Journal of Environmental Chemical Engineering

journal homepage: www.elsevier.com/locate/jece

# Encapsulation and controlled release of isothiazolinones in zeolite NaY (FAU)

Lucas Mardones [a], Leyanet Barberia Roque [b], María S. Legnoverde [a,*], Nicola Gargiulo [c,d], Natalia Bellotti [b], Elena I. Basaldella [a]

[a] Centro de Investigación y Desarrollo en Ciencias Aplicadas (CINDECA), Facultad de Ciencias Exactas, Universidad Nacional de La Plata – CONICET, Calle 47 N°257, B1900AJK La Plata, Argentina
[b] Centro de Investigación y Desarrollo en Tecnología de Pinturas (CIDEPINT-CONICET-CICPBA-UNLP), Av. 52 e/ 121 y 122, B1900AYB La Plata, Argentina
[c] ACLabs - Laboratori di Chimica Applicata, Dipartimento di Ingegneria Chimica, dei Materiali e della Produzione Industriale, Università di Napoli Federico II, P.le V. Tecchio 80, 80125 Napoli, Italy
[d] CeSMA – Centro di Servizi Metrologici e Tecnologici Avanzati, Università di Napoli Federico II, Corso N. Protopisani, 80146 Napoli, Italy

ARTICLE INFO

Editor: V. Victor

*Keywords:*
Zeolite
Biocide
Isothiazolinones
Adsorption
Controlled release

ABSTRACT

NaY zeolite, an ordered, large pore molecular sieve pertaining to the FAU zeolite structural group, was studied as a novel matrix for the efficient preparation of a supported isothiazolinone-based biocide, and the results were compared to those corresponding to mesoporous silicas. To analyze the possibility of reducing the biocide ecotoxicity by encapsulation, a commercial biocide used for latex preservation (CMIT/MIT) was incorporated in the NaY zeolite structure by using two different methodologies: equilibrium adsorption (Zeo/Bio sample) and impregnation by total wetting (Zeo/Impreg sample). In the corresponding release tests, despite the large difference in the initial biocide amount released, the shape of the curve is nearly the same for both methods. Microbiological tests against fungi and bacteria were performed. The obtained results were compared to those previously obtained using mesoporous ordered silica SBA-15 and mesoporous foam MCF matrices (mesoporous/biocide samples named SBA-15/Bio, SBA-15/Impreg and MCF/Bio and MCF/Impreg respectively). For the Staphylococcus aureus the results from agar well diffusion assay shows that the inhibition zone is about 64 mm for Zeo/Impreg and about 55 mm for Zeo/Bio. As regards all the other materials, the inhibition zone does not exceed 46 mm. In the case of Escherichia coli, Zeo/Bio and Zeo/Impreg have an inhibition zone of about 43 and 37 mm, respectively. No one of the other materials shows an inhibition zone larger than 30 mm. Zeo/Impreg showed a greater inhibition zone against fungi (47 mm versus Chaetomium globosum and 53 mm versus Alternaria alternata, respectively) than SBA-15 and MCF impregnated with biocide.

## 1. Introduction

Biocides are antimicrobial agents incorporated in different coating formulations used to prevent microbial deterioration of materials and products such as plastics, paint, paper, textiles, hygienic surfaces and floors. It is well known that, in coated surfaces, the presence of biocide molecules inhibits the growth of microorganisms, thus preserving both the performance of the substrate material and its aesthetic appearance. The common way to prevent biological growth on coated materials is the direct addition of the liquid biocidal substances to the coating formulation. A drawback of this procedure is related to the fact that biocides can eliminate the presence of microorganisms and prevent their recurrence but only for relatively short periods of time. The release of the biocide is frequently uncontrolled, resulting in short biocidal protection and large emissions to the environment.

During a long period of time, a variety of substances have been used as biocides and antifouling agents with excellent outcomes. Nevertheless, some of them adversely affect the environment. For example, tributyltin, usually used in antifouling paints, leads to the appearance of malformations in non-target organisms [1,2]. Moreover, copper compounds, which are biocides commonly used for antifouling marine coatings, bioaccumulates in the internal organs of many species [3]. As biocides undoubtedly are harmful substances for human health and environment, a sensible reduction of the used amount of the biocidal

* Corresponding author.
*E-mail address:* mslegnoverde@quimica.unlp.edu.ar (M.S. Legnoverde).

https://doi.org/10.1016/j.jece.2022.107277
Received 11 November 2021; Received in revised form 5 January 2022; Accepted 24 January 2022
Available online 5 February 2022

component in a coating formulation as well as a longer duration of the biocidal action would be desirable.

Isothiazolinones are fast-acting biocides: in particular, the chemical mixture 5-chloro-2-methyl-4-isothiazolin-3-one/2-methyl-4-isothiazolin-3-one (CMIT/MIT) has been widely used as disinfectant additive for manufacturing a variety of products, i.e., household cleaning and personal care products [4–6].

Moreover, CMIT/MIT is commonly used in the paint industry for the formulation of hygienic paints. CMIT/MIT is very effective for preventing microbial growth (bacteria, fungi and yeasts), being also able to control the development of biofilms. The most frequently used commercial formulation of isothiazolinones (BIO) for the preparation of waterborne paints consists of an aqueous solution containing 1.5 wt% of CMIT and MIT in a CMIT/MIT = 3 wt ratio [7]. The CMIT/MIT mixture can cause skin irritation and allergies [8–11] and could present environmental risks [4], being its concentration in commercial products strictly regulated to 15 ppm in the European Union and South Korea [12–14].

Recent studies on the encapsulation of biocides in nanoporous inorganic materials and their use in the formulation of coatings indicate that this procedure could be suitable to obtain a long-term protection of those components of the paints susceptible to microbiological attacks.

When the liquid CMIT/MIT biocide solution is directly added to the paint formulation, three mechanisms for the transport of biocide molecules in exposed painted surfaces have been suggested, being the control exerted by the diffusion through the water-filled pores [15]. In the case of the CMIT/MIT biocide mixture, its low hydrophobicity and high water solubility (compared to those shown by the different biocides used nowadays) are the most important parameters that favor leaching. For this reason, biocide encapsulation inside inorganic porous matrices offers the possibility of an additional barrier that could effectively retard leaching. This fact also implies the controlled antimicrobial action of the adsorbate, avoiding the presence of high initial concentrations of biocide [16–20]. As a consequence, reducing the quantities of biocide needed to obtain an efficient antimicrobial effect has the added benefit of reducing the amount of chemicals released into the environment and thus any potential hazardous unwanted consequences.

In a previous work, we achieved the encapsulation of commercial biocides in mesoporous materials such as SBA-15 and MCF [17,21]. These inorganic silicas were selected because of their successful use as matrices for the controlled delivery of pharmaceutics [22–24]. On these grounds, the addition to paint formulations of a commercial biocide encapsulated in the aforementioned mesoporous matrices was successfully carried out and the corresponding biocidal activity was tested against different microorganisms [25]. According to the obtained results, mesoporous silicas represent a promising approach to encapsulate antimicrobials that enable long-lasting, controlled leaching. However, despite the excellent properties of these materials, their manufacturing cost is usually high. On this basis, and taking into account the sizes of CMIT and MIT molecules, i.e., 0.577 × 0.378 nm and 0.521 × 0.378 nm, respectively (Fig. 1) [21], it can be inferred that such biocide compounds could be adsorbed within the pore structure of zeolites such as those belonging to the FAU type.

In such zeolitic structure, each unit cell contains eight supercages, eight sodalite cages and 16 hexagonal prisms (Fig. 2). The diameters of the 6-ring windows of the sodalite cages and of the 12-ring windows of the supercages are about 2.4 Å and 7.4 Å, respectively. According to the aforementioned dimensions and regarding the zeolite structure as a molecular sieve, water molecules have no steric hindrance for entering both the supercages and the sodalite cages, while CMIT/MIT molecules may only be accommodated in the supercages. On this basis, this paper reports the use of NaY zeolite as a cost-efficient matrix for supporting the BIO commercial biocide, and its performance was evaluated both in terms of biocide adsorption/desorption processes and antimicrobial activity against bacteria (i.e., Staphylococcus aureus and Escherichia

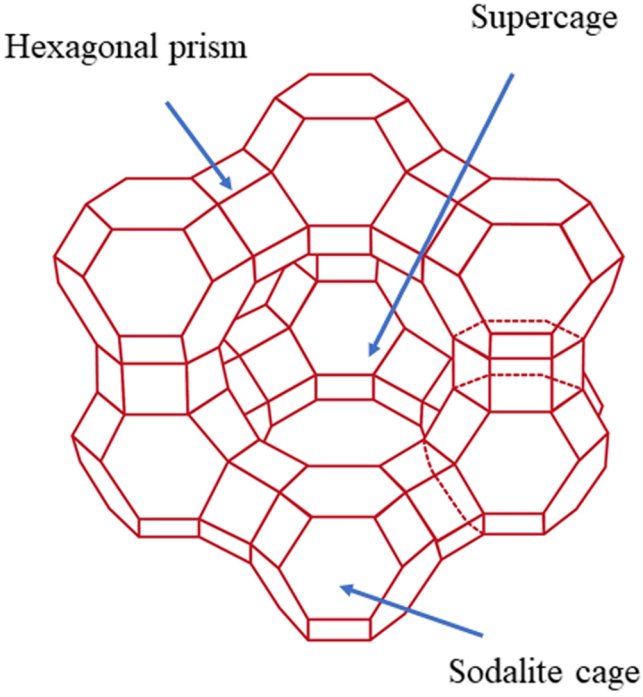


**Fig. 2.** Structure of faujasite, showing the structure of the supercage, the sodalite cage and the hexagonal prism.

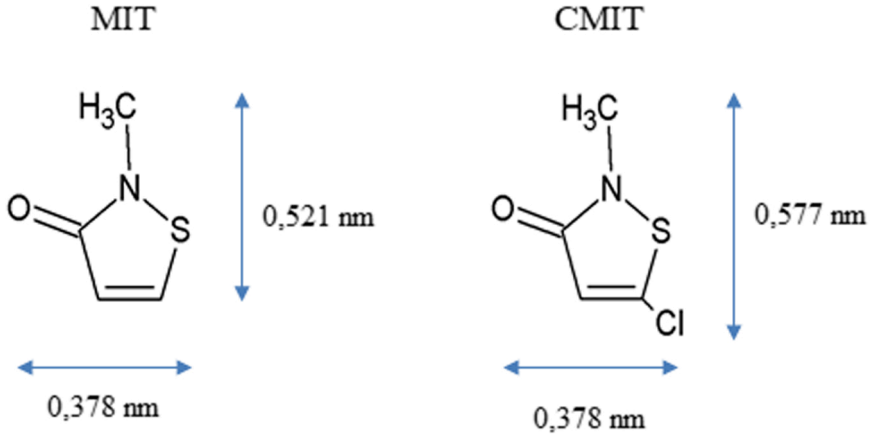


**Fig. 1.** 2D appearances of biocide molecules with relative dimensions.

coli) and fungi (i.e., Chaetomium globosum and Alternaria alternata). A comparison with the efficiency shown by mesoporous materials in similar conditions is also reported.

## 2. Materials and methods

### 2.1. Synthesis of zeolite Y

The hydrothermal synthesis of zeolite NaY was carried out in a closed polypropylene vessel, at 100 °C, without agitation. The raw materials used were NaOH (CarloErba, analytical reagent), commercial sodium aluminate (36.5% w/w $Al_2O_3$, 29.6% w/w $Na_2O$, 33.9% w/w $H_2O$), sodium silicate (9.2% $Na_2O$, 26.8% $SiO_2$, 64% $H_2O$) and distilled water. The synthesis of the zeolite was carried out following the procedure described by Robson [26]. The formula unit of the synthesized material is $Na_{56}[Al_{56}Si_{136}O_{384}]$: 250 $H_2O$. The obtained solid was labeled as ZeoY.

### 2.2. Preparation of the biocide loaded samples

Two methods for preparing the biocide/support composite were used.

#### 2.2.1. Adsorption at equilibrium

Batch equilibrium tests were carried out for CMIT/MIT adsorption on the prepared zeolite under stirring. Sample fractions of the liquid phase were withdrawn at different times and then re-added to the batch in order to precisely determine the residual concentration at the sampling time and avoid any perturbation that could influence the equilibrium conditions at the end of the experiments. The CMIT/MIT initial concentration was fixed at 200 mg/mL, whereas other parameters such as adsorbent mass (0.2 g), stirring rate (120 rpm), solution volume (100 mL) and solution temperature (25 °C) were kept constant. At the end of the adsorption run, the biocide-loaded zeolite was dried at 25 °C for 24 h. Dry solid product (sample Zeo/Bio) was then stored until further use, whereas the collected eluate containing non-adsorbed biocide was used for the estimation of biocide loading content of the zeolite by using an UV–Vis spectrophotometer (PerkinElmer Lambda 35). The collected eluate containing non-retained biocide was scanned at 274 nm, i.e., the characteristic absorbance wavelength of CMIT/MIT. The amount of CMIT/MIT adsorbed at equilibrium, $q_e$ (mg/g), was calculated by:

$$q_e = (C_o - C_e)V/\ W$$

where $C_o$ is the initial concentration of biocide in the solution (expressed in mg/mL), $C_e$ is the solution concentration of biocide at the equilibrium (in mg/mL), V is the solution volume of the batch (in mL) and W is the adsorbent weight (expressed in g).

#### 2.2.2. Incipient wetness

CMIT/MIT was added dropwise to the sample, until total wetting of the solid. The impregnated sample was dried at room temperature. The resulting solid was called Zeo/Impreg.

### 2.3. Characterization

The synthesized NaY zeolite was characterized by X-ray diffraction (XRD) using a Philips PW 1732/10 equipment (CuKα radiation, scanning speed: 2°/min). The size and morphology of the zeolite particles were observed by scanning electron microscopy (SEM) using a Philips 505 instrument. The material employed for sputter coating SEM samples was Au. Nitrogen adsorption–desorption isotherms were determined with a Micromeritics ASAP 2020 instrument at the temperature of liquid nitrogen (−196 °C). Before adsorption, samples were outgassed by heating at 100 °C in vacuum (pressure lower than $3 \times 10^{-2}$ mm Hg) for 12 h. The models employed for calculating the specific surface area were the Langmuir and the Brunauer–Emmett–Teller (BET) ones. The total pore volume was calculated by the Gurvich's rule at $p/p_0 = 0.9$, while the micropore volume was calculated by the t-plot method using the thickness equation defined by Kruk, Jaroniec and Sayari [27]. Fourier transform infrared (FT-IR) spectra were obtained with a Shimadzu IRAffinity-1 spectrometer: samples were pelletized in KBr, and the measurements were performed in the 400–4000 $cm^{-1}$ wavenumber range.

### 2.4. Biocide release experiments

The release kinetics measurements of CMIT/MIT from Zeo/Bio and Zeo/Impreg were performed in aqueous media at 25 °C. For this purpose, 0.2 mg of the biocide-loaded adsorbent was soaked in 100 mL of water under stirring.

Once the release test was completed (biocide concentration kept constant in the release medium), the solid was recovered by filtration and dried at room temperature. Then, the obtained samples (Zeo/Bio2 and Zeo/Impreg2) were put again in a biocide-free liquid medium, in order to measure the feasibility of a further biocide release.

In all cases, the corresponding released concentration as a function of time was determined by UV–Vis spectroscopy (PerkinElmer Lambda 35) at 274 nm.

### 2.5. Antimicrobial activity

Agar well diffusion method was performed in order to assess the antibacterial and antifungal activity of the prepared biocide-loaded samples [28]. The investigated bacterial strains were Staphylococcus aureus (ATCC 6538) and Escherichia coli (ATCC 11229), while the investigated fungi were Chaetomium globosum (KU936228) and Alternaria alternata (KU936229). For comparative purposes, other porous materials besides Zeo/Bio and Zeo/Impreg samples were evaluated. The same two methods for incorporating biocide molecules as described in Section 2.2 were used for SBA-15 and MCF mesoporous silicas samples. The latter materials have already been microbiologically tested in a previous work by using a different methodology [25]. The mesoporous silica samples were named SBA/Bio and MCF/Bio whereas the biocide was incorporated by the equilibrium adsorption method, while the solids submitted to biocide impregnation by incipient wetness were named SBA/Impreg and MCF/Impreg. Pristine porous supports that were not loaded with biocide (ZeoY, MCF and SBA-15) were also tested. In all cases, triplicates of each sample were performed. 7 mm diameter wells were built in seeded agar plates and filled with 20 mg of the tested samples. The culture media used for bacteria and fungi were Luria Bertani Agar (LBA) and Malt Extract Agar (MEA), respectively. The inoculum was adjusted to 106 UFC/mL for bacterial strains and to 105 spores/mL for the fungi. The plates were incubated for 24 h at 30 °C for bacterial strains and for 48 h at 28 °C for fungi. Eventually, inhibition zone diameters were measured: diameters $< 7$ mm were considered indicative of the absence of antibacterial and antifungal activity. Diameters $> 7$ mm were considered indicative of the presence of antibacterial and antifungal activity, while diameters around 7 mm were considered only indicative of the presence of antifungal activity.

The corresponding statistical parameters were calculated using the Infoestat program. Statistical analysis of the results was carried out using a parametric method of analysis of variances (ANOVA) with $\alpha = 0.05$ and the Tukey test for comparison of means.

## 3. Results and discussion

### 3.1. Characterization

Fig. 3a shows the XRD pattern of the synthesized zeolite: the diffraction peaks corresponding to NaY zeolite as reported in the

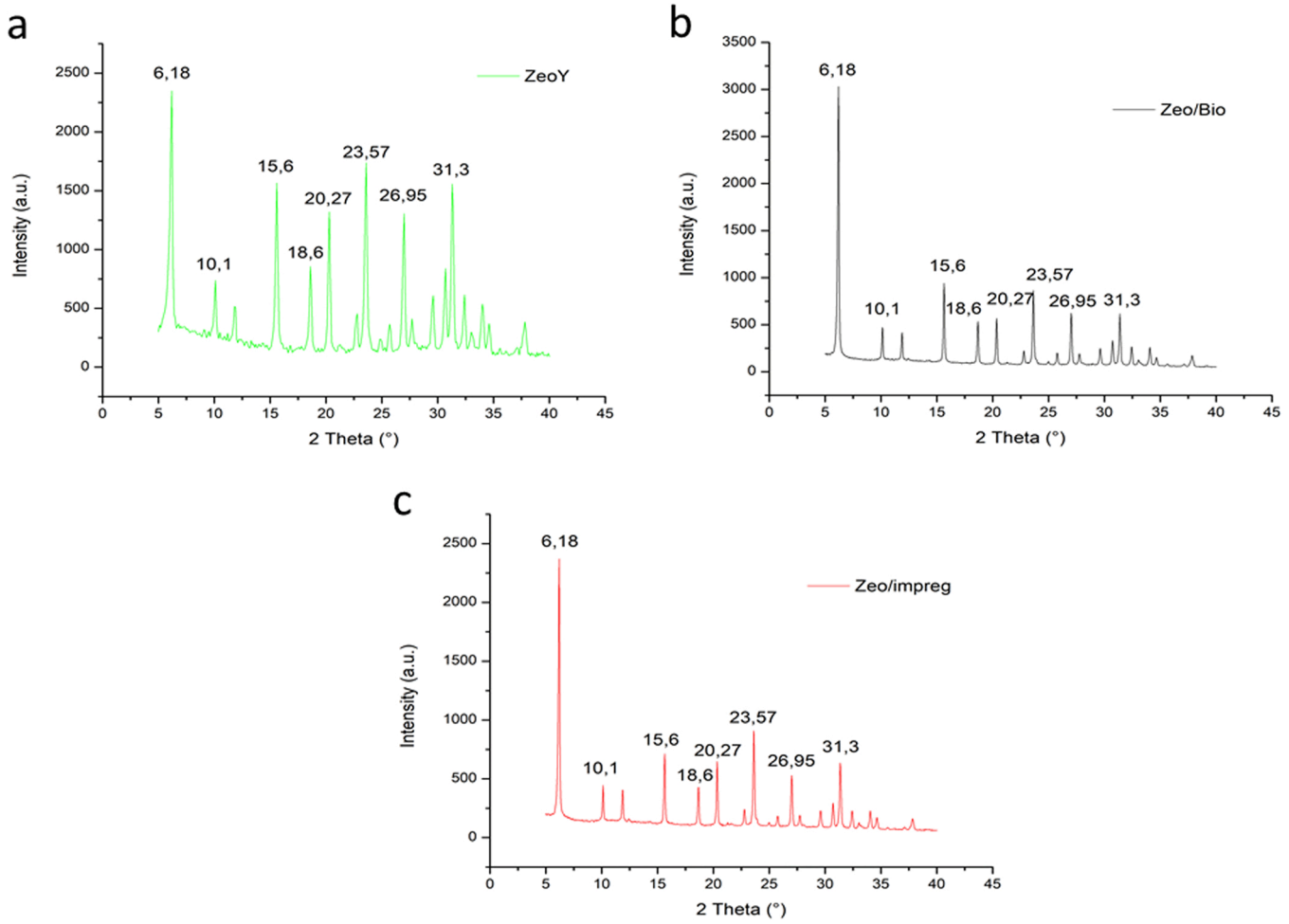


**Fig. 3.** X-ray diffraction patterns of (a) ZeoY, (b) Zeo/Bio and (c) Zeo/impreg.

literature are clearly observed [29]. All the same peaks appear in the biocide-loaded samples (Fig. 3b and c). In the latter case, no additional peak is detected. However, a decrease in intensity of almost all peaks is observed after biocide incorporation.

Fig. 4a shows a SEM image of the synthesized zeolite, where the typical morphology of this material can be observed, consisting of particles of about 0.3–0.5 μm originating from compenetrating tetrahedral crystals [30]. Fig. 4b and c show the SEM image of Zeo/Bio and Zeo/Impreg, respectively. It can be observed that, with respect to ZeoY, there is no change in morphology.

ZeoY, Zeo/Bio and Zeo/Impreg were analyzed by FTIR (Fig. 5). The characteristic bands of FAU structures are observed in the spectrum of ZeoY [29]. Moreover, in the spectra corresponding to loaded materials (Zeo/Bio and Zeo/Impreg), the absorption bands of the isothiazolinone structure are clearly detected. Indeed, bands at 2940, 2890 and 886 $cm^{-1}$ (assigned to the C-H stretch vibration), in the range of 1450–1390 $cm^{-1}$ (attributable to the C-H flexion) and at 600 $cm^{-1}$ (i.e., the band corresponding to the stretching of C-Cl) can be observed [17, 25,31]. These results prove that biocide molecules retain their chemical integrity after being adsorbed.

The $N_2$ adsorption-desorption isotherms of ZeoY and Zeo/Bio are reported in Fig. 6 (for the Zeo/Impreg sample, the $N_2$ adsorption-desorption test was not significant because the pores were entirely filled with biocide molecules). Both isotherms, as can be expected from microporous zeolitic structures, fall into the IUPAC Type I classification [32]. The textural characteristics of the prepared solids are summarized in Table 1. The Langmuir specific surface area values were 525 $m^2/g$ for ZeoY and 441 $m^2/g$ for Zeo/Bio, while the corresponding BET specific surface areas proved to be 473 and 386 $m^2/g$, respectively. The total pore volume of ZeoY is 0.194 $cm^3/g$, whereas it is 0.162 $cm^3/g$ for Zeo/Bio. Actually, loading ZeoY with biocide molecules caused a decrease of the total pore volume of about 0.03 $cm^3/g$. Contextually, the micropore volume of ZeoY decreased from 0.177 to 0.143 $cm^3/g$, i.e., the loading procedure with biocide molecules also lowered the micropore volume of about 0.03 $cm^3/g$. This can be considered an indirect proof that biocide molecules are specifically loaded inside the micropores of the zeolitic support.

### 3.2. Adsorption and controlled release

After adsorption, different biocide amounts were found in the samples. For Zeo/Bio, the percentage of adsorbed biocide turned out to be 24.2% of the amount initially present in the solution, while the biocide content present in the Zeo/Impreg sample is 1.9 g per gram of zeolite.

The percentages of adsorbed biocide (adsorption at equilibrium) by the mesoporous materials reported in a previous work were 18% and 27% for SBA-15 and MCF, respectively [25]. As both materials are quite similar in nature (pure silica networks), their dissimilar adsorbed quantities were attributed to differences in textural properties [17]. In the case of the Zeo/Bio, the percentage of adsorbed biocide is 24.2%, although the pore diameters are smaller than those present in mesoporous silicas. The higher amount of biocide adsorbed by the zeolite with respect to those adsorbed by the examined mesoporous materials seems to be related to the corresponding surface areas. For comparison, the more important textural properties of the latter materials and their biocide adsorption capacity are summarized in Table 2.

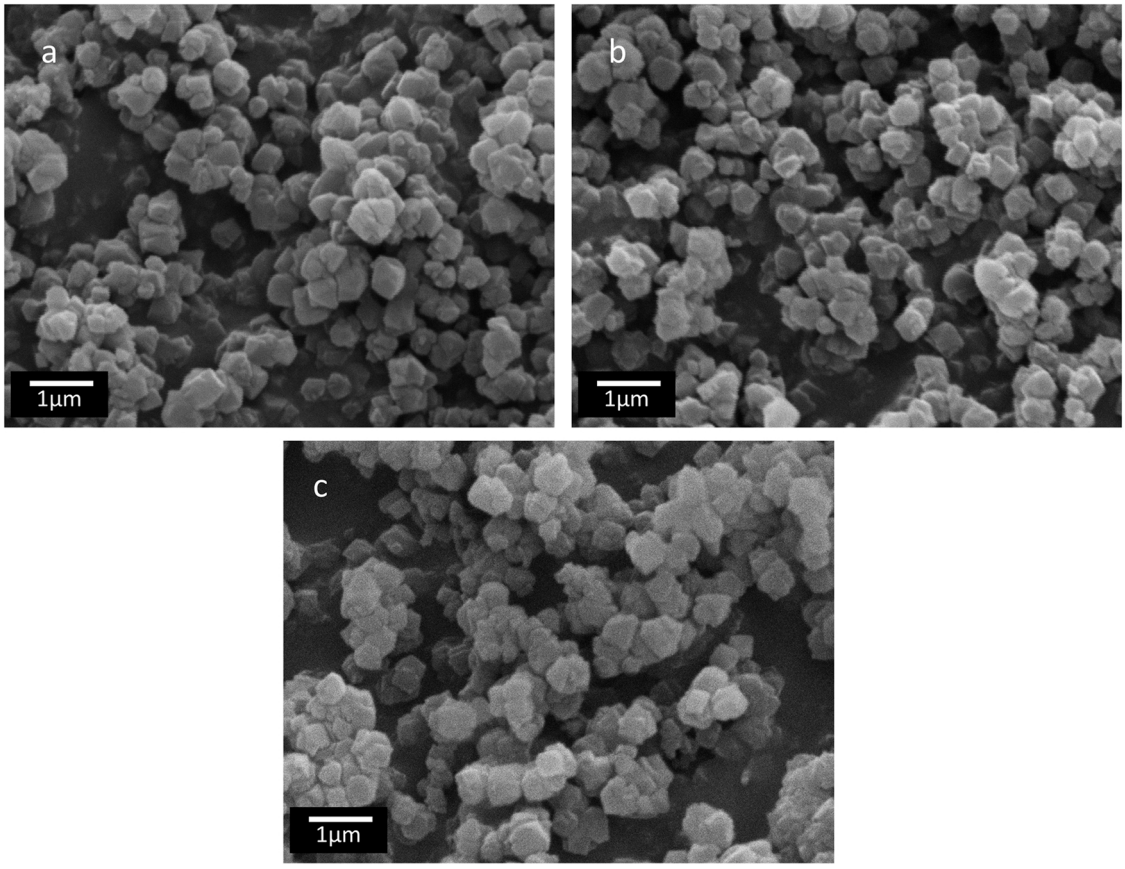


**Fig. 4.** SEM micrographs of (a) ZeoY (magnification × 10,000), (b) Zeo/Bio (magnification × 10,000) and (c) Zeo/Impreg (magnification × 10,000).

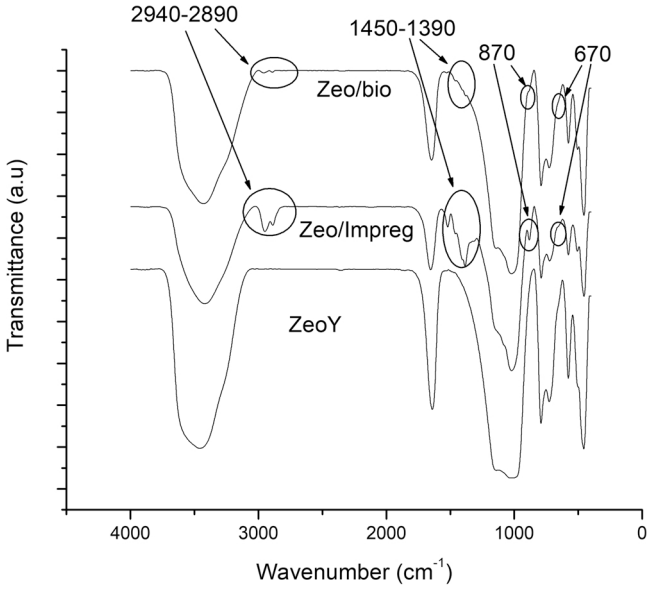


**Fig. 5.** FTIR Spectra of ZeoY, Zeo/Bio and Zeo/Impreg.

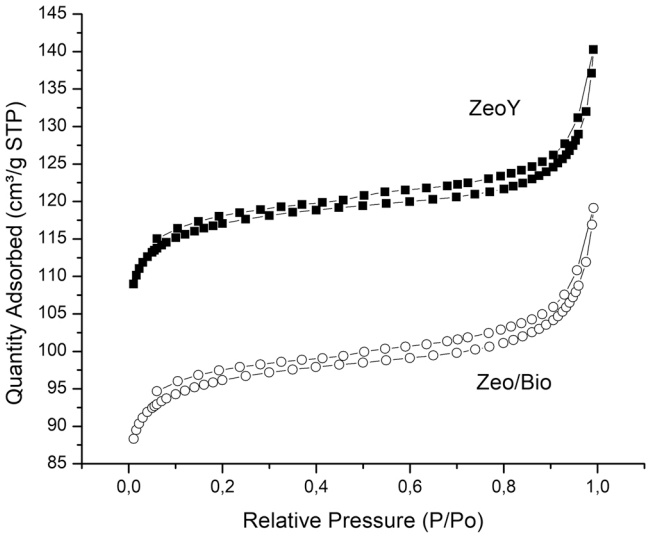


**Fig. 6.** $N_2$ adsorption-desorption isotherms of ZeoY and Zeo/Bio.

Fig. 7 shows the biocide release profiles for Zeo/Bio and Zeo/Impreg samples over a period of 15 days. The biocide amounts released from the two samples are significantly different. An initial, steep release of biocide from both samples occurred at short times (<1 h), while the percentage of released biocide after 15 days is 51 wt% for Zeo/Impreg and 8 wt% for Zeo/Bio. Despite the large difference in the released biocide amount, the shape of the curve is nearly the same for both

**Table 1**
Textural properties of ZeoY before and after biocide adsorption.

| Sample | $S_{Langmuir}$ ($m^2/g$) | $S_{BET}$ ($m^2/g$) | Total Pore Vol. ($cm^3/g$) | t-plot Microp. Vol. ($cm^3/g$) |
|---|---|---|---|---|
| ZeoY | 525 | 473 | 0.194 | 0.177 |
| Zeo/Bio | 441 | 386 | 0.162 | 0.143 |

**Table 2**
Textural properties of mesoporous materials before and after biocide adsorption.

| Sample | $S_{BET}$ ($m^2$/g) | Total Pore Vol. ($cm^3$/g) | Loaded % |
|---|---|---|---|
| SBA-15 | 578 | 0.48 | |
| MCF | 713 | 0.71 | |
| SBA/Bio | 247 | 0.34 | 18 |
| MCF/Bio | 261 | 0.73 | 27 |

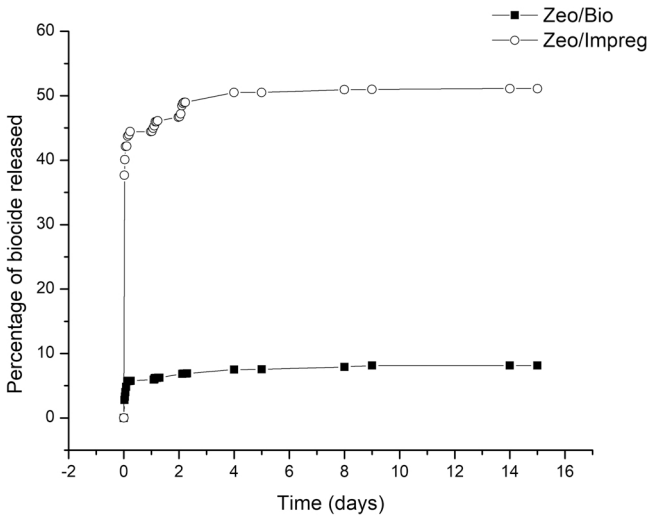


**Fig. 7.** Biocide release profiles from Zeo/Bio and Zeo/Impreg.

samples. As the biocide loading is different in the two samples, the adsorbate fraction remaining weakly adsorbed to the solid in the Zeo/Impreg sample should be notoriously higher than that in Zeo/Bio, which would account for the dissimilarity in the amounts of biocide released by both samples at the beginning of the delivery.

Analyzing the biocide release profiles of Zeo/Bio2 and Zeo/Impreg2 (Fig. 8), a behavior similar to that shown by the first release test is observed, although the amounts released by Zeo/Bio2 and Zeo/Impreg2 are considerably lower than those released by Zeo/Bio and Zeo/Impreg. Nevertheless, the supposedly exhaust carriers prove themselves to be able to release an additional fraction of their payload once put again in a biocide-free liquid medium.

Compared to mesoporous silica [17], zeolite-based samples show a slower release rate in the second stage of their release profiles. The

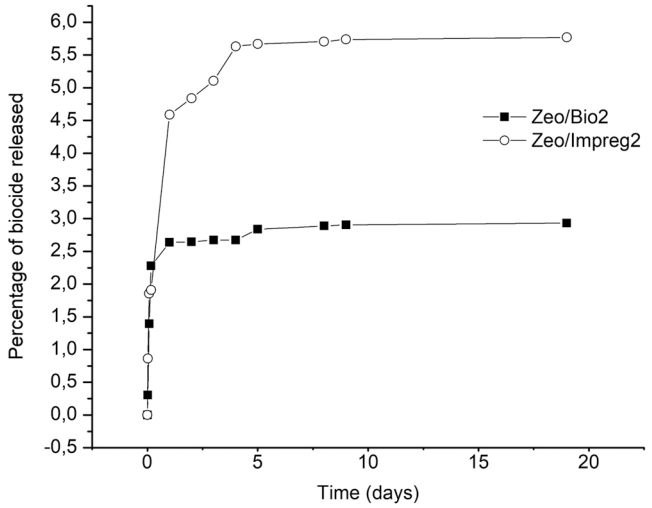


**Fig. 8.** Biocide release profiles from Zeo/Bio2 and Zeo/Impreg2.

second stage of the delivery curve is attributed to the desorption of the biocide molecules localized in the microporous channels. If the interaction between the biocide molecules and the zeolite framework is stronger than the interaction between the biocide molecules and the mesoporous materials, then the release will be more difficult. Indeed, adsorption phenomena on zeolitic surfaces (that contains both Al and Si) could be very distinct than those on pure silica matrices. In other words, the diffusive processes that occur in zeolites are different from those that occur in mesoporous solids not only because of different pore sizes, but also because of very different adsorbent-adsorbate interactions. The arrangements of aluminate and silicate tetrahedra in the zeolite framework, as well as the presence of the alkaline cations, define a cage potential and a particular crystal field distribution that determine an electrostatic adsorbent-adsorbate interaction. In NaY zeolite, the framework surface is essentially made of exposed oxygen atoms. The Si and Al atoms are located below such oxygen atoms, which are fully accessible to adsorbate molecules. Moreover, these negatively charged oxygen atoms, whose polarizability depends on the presence of Al and Si atoms, regulate the van der Waals adsorbent-adsorbate interactions. It is also known that not all the compensating Na cations are located in accessible sites. Then, the positive charge of the compensating cations [33,34] and the electrophilic nature of the biocide molecules are also responsible for the attraction forces dominating the biocide retention inside the zeolite framework [35]. On this basis, the interaction between biocide molecules and zeolite surface is supposed to be stronger than the interaction between biocide molecules and the surface of mesoporous materials, allowing a higher biocide retention and thus hindering its release.

### 3.3. Antimicrobial activity test

The results from agar well diffusion assay are shown in Fig. 9. Generally, bacteria and fungi show significantly different sensitivities to the examined products, S. aureus being the most sensitive in the first group and A. alternata in the second one. Non-loaded MCF and SBA-15 have some activity against S. aureus, but it is significantly lower than that of same solids loaded with biocide. Significant differences are also observed in the light of the different methods used for the incorporation of biocide molecules in the solids. Indeed, Zeo/Bio generally shows smaller inhibition zones when compared with Zeo/Impreg. Wider inhibition zones can be related to a higher lixiviation of the biocide from the sample. Zeo/Bio and Zeo/Impreg show a wider inhibition zone for both bacteria with respect to all the biocide-loaded SBA-15 and MCF samples. As regards both the tested fungi, Zeo/Impreg performs better than Zeo/Bio, SBA/Bio, SBA/Impreg and MCF/Impreg.

Fig. 10 shows photographic images of the Petri dishes used for the microbiological tests involving Zeo/Bio and Zeo/Impreg. These images were taken at 24 h for the assays against bacteria and at 48 h for the assays against fungi. It can be noted that the pristine zeolite has no inhibition effect against microorganisms and that Zeo/Impreg generally shows the best performance against microbiological agents.

## 4. Conclusions

The results showed that CMIT/MIT biocide mixture retains its chemical integrity after being adsorbed inside the pores of a FAU-type zeolite. The incorporation of CMIT/MIT in zeolite NaY could be advantageous because of the proved feasibility of controlling the biocide release profile by changing the structure of the carrier. Compared to mesoporous silicas, the structure of zeolite NaY would allow maintaining a slower and sustained biocide leaching. The chosen zeolite was loaded with CMIT/MIT by two different methodologies and showed a better activity against the tested bacteria with respect to mesoporous materials. The biocide-impregnated zeolite also showed better inhibition properties against fungi with respect to biocide-impregnated SBA-15 and MCF. These findings claim a deeper insight into the possibilities

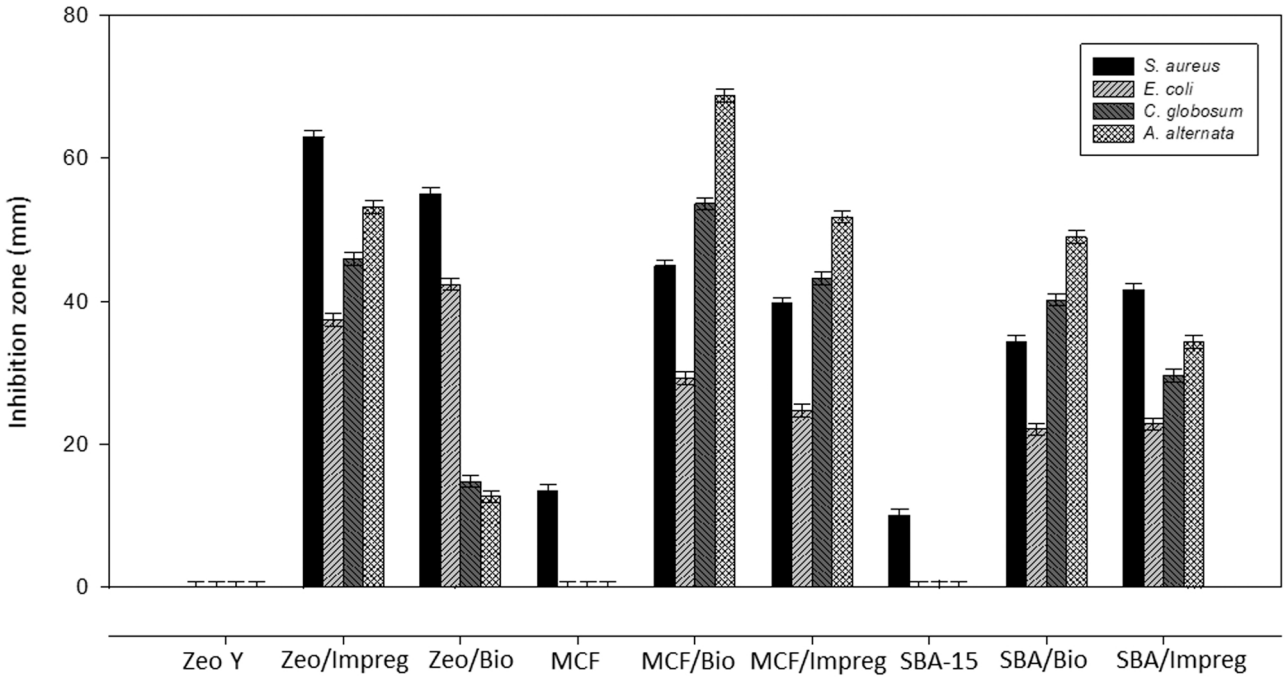


**Fig. 9.** Diameters of inhibition zones by agar diffusion tests against bacterial and fungal strains for the tested samples.

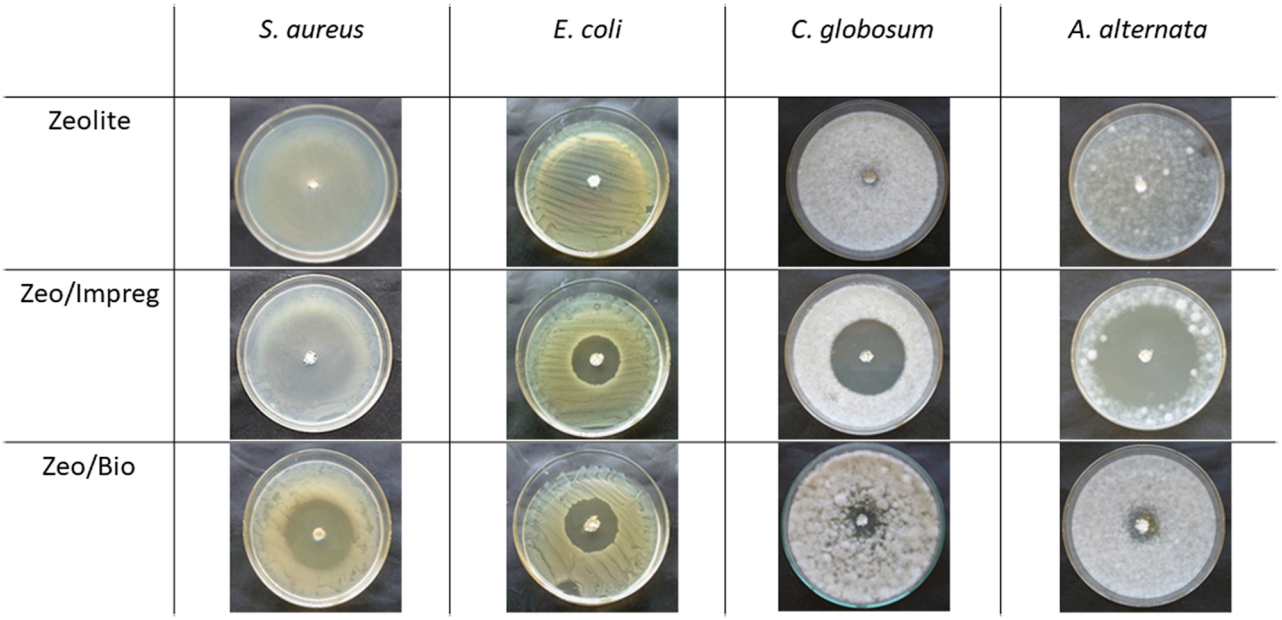


**Fig. 10.** Diffusion assay plates containing the tested samples.

of preserving the activity of biocidal additives and thus prolonging the protection paints in liquid state. Indeed, it seems that it is possible to design a microbiocidal active formulation that provides slow-release by simply adsorbing the active substance onto the surface of a carrier (i.e., a zeolite) showing a relatively low biocide desorption rate. Moreover, the same carrier could also act as a filler for the preparation of coatings.

## Funding

The researches leading to these results receive funding from ANPCyT, Argentina under grant Project PICT 2017-2931.

## CRediT authorship contribution statement

**Lucas Mardones:** Methodology, Investigation, Writing – original draft. **Leyanet Barberia Roque:** Methodology, Investigation. **María S. Legnoverde:** Conceptualization, Writing – original draft, Writing – review & editing. **Nicola Gargiulo:** Investigation, Formal analysis, Writing – original draft. **Natalia Bellotti:** Investigation, Writing – original draft. **Elena I. Basaldella:** Conceptualization, Writing – original draft, Writing – review & editing, Supervision.

## Declaration of Competing Interest

The authors declare that they have no known competing financial

interests or personal relationships that could have appeared to influence the work reported in this paper.

## Acknowledgements

The authors acknowledge the financial support received from CONICET, CIC-PBA, UTN and ANPCyT for their financial support.

## References

[1] M. Champ, A review of organotin regulatory strategies, pending actions, related costs and benefits, Sci. Total Environ. 258 (2000) 21–71.
[2] D. Meseguer Yebra, S. Kiil, K. Dam-Johansen, Antifouling technology—past, present and future steps towards efficient and environmentally friendly antifouling coatings, Prog. Org. Coat. 50 (2004) 75–104.
[3] M. Loureiro, M. Vale, A. De Schrijver, J. Bordado, E. Silva, A. Marques, Hybrid custom-tailored sol-gel derived microscaffold for biocides Immobilization, Microporous Mesoporous Mater. 261 (2018) 252–258.
[4] A. Rafoth, S. Gabriel, F. Sacher, H. Brauch, Analysis of isothiazolinones in environmental waters by gas chromatography–mass spectrometry, J. Chromatogr. A 1164 (2007) 74–81.
[5] T.Y. Kwon, J. Jeong, E. Park, Y. Cho, D. Lim, U.H. Ko, J.H. Shin, J. Choi, Physical analysis reveals distinct responses of human bronchial epithelial cells to guanidine and isothiazolinone biocides, Toxicol. Appl. Pharmacol. 424 (2021), 115589.
[6] Z.W. Yang, W.L. Wang, M.Y. Lee, Q.Y. Wu, Y.T.Guan Synergistic, effects of ozone/peroxymonosulfate for isothiazolinone biocides degradation: kinetics, synergistic performance and influencing factors, Environ. Pollut. 294 (2022), 118626.
[7] N. Hunziker, The “isothiazolinone story”, Dermatology 184 (1992) 85–86.
[8] E. Garcia-Hidalgo, D. Schneider, N. von Goetz, C. Delmaar, M. Siegrist, K. Hungerbühler, Aggregate consumer exposure to isothiazolinones via household care and personal care products: Probabilistic modelling and benzisothiazolinone risk assessment, Environ. Int. 118 (2018) 245–256.
[9] M. Tokunaga, H. Fujii, K. Okada, Y. Kagemoto, T. Nomura, M. Tanioka, Y. Matsumura, Y. Miyachi, Occupational airborne contact dermatitis by isothiazolinones contained in wall paint products, Allergol. Int. 62 (2013) 395–397.
[10] M. Ruiz Montoya, I. Giraldez, E. Morales, R. Estevez Brito, J.M. Rodríguez Mellado, Electrochim. Acta 337 (2020), 135770.
[11] M. Giácaman-von der Weth, A. Pérez-Ferriols, C. Sierra-Talamantes, V. Zaragoza-Ninet, Actas Dermosifiliog 109 (2018) 291–292.
[12] Cosmetics: Regulation (EC) No. 1223/2009 of the European Parliament and of the Council of 30 November 2009 on cosmetic products (recast), Off. J. Eur. Union L342 ,2009, 59.
[13] G. Davison, B. Lane, Paints: Additives in Water-borne Coatings, The Royal Society of Chemistry, London, 2003.
[14] T. Kang, C. Jin, S. Lee, I. Choi, Dual mode rapid plasmonic detections of chemical disinfectants (CMIT/MIT) using target-mediated selective aggregation of gold nanoparticles, Anal. Chem. 92 (2020) 4201–4208.
[15] C. Paijens, A. Bressy, B. Frère, R. Moilleron, Biocide emissions from building materials during wet weather: identification of substances, mechanism of release and transfer to the aquatic environment, Environ. Sci. Pollut. Res. 27 (2020) 3768–3791.
[16] C. Dresler, M. Saladino, C. Demirbag, E. Caponetti, D. Martino, R. Alduina, Development of controlled release systems of biocides for the conservation of cultural heritage, Int. Biodeterior. Biodegrad. 125 (2017) 150–156.
[17] L. Mardones, M. Legnoverde, A. Pereyra, E. Basaldella, Long-lasting isothiazolinone-based biocide obtained by encapsulation in micron-sized mesoporous matrices, Prog. Org. Coat. 119 (2018) 155–163.
[18] G. Sørensen, A.L. Nielsen, M.M. Pedersen, S. Poulsen, H. Nissen, M. Poulsen, S. D. Nygaard, Controlled release of biocide from silica microparticles in wood paint, Prog. Org. Coat. 68 (2010) 299–306.
[19] J. Eversdijk, S.J.F. Erich, S.P.M. Hermanns, O.C.G. Adan, M. De Bolle, K. de Meyer, D. Bylemans, M. Bekker, A.T. ten Cate, Development and evaluation of a biocide release system for prolonged antifungal activity in finishing materials, Prog. Org. Coat. 74 (2012) 640–644.
[20] J. Bergek, M. Andersson Trojer, A. Mok, L. Nordstierna, Controlled release of microencapsulated 2-n-octyl-4-isothiazolin-3-one from coatings: effect of microscopic and macroscopic pores, Colloids Surf. A 458 (2014) 155–167.
[21] L. Mardones, M. Legnoverde, S. Simonetti, E. Basaldella, Theoretical and experimental study of isothiazolinone adsorption onto ordered mesoporous silica, Appl. Surf. Sci. 389 (2016) 790–796.
[22] M. Legnoverde, S. Simonetti, E. Basaldella, Influence of pH on cephalexin adsorption onto SBA-15 mesoporous silica. Theoretical and experimental study, Appl. Surf. Sci. 300 (2014) 37–42.
[23] M. Legnoverde, I. Jiménez-Morales, E. Rodríguez-Castellón, A. Jiménez-Morales, E. Basaldella, Modified silica matrices for controlled release of cephalexin, Med. Chem. 9 (2013) 672–680.
[24] E. Basaldella, M. Legnoverde, Functionalized silica matrices for controlled delivery of cephalexin, J. Sol-Gel Sci. Technol. (2010) 191–196.
[25] L. Mardones, M. Legnoverde, J. Monzón, N. Bellotti, E. Basaldella, Increasing the effectiveness of a liquid biocide component used in antifungal waterborne paints by its encapsulation in mesoporous silicas, Prog. Org. Coat. 134 (2019) 145–152.
[26] H. Robson, Verified Syntheses of Zeolitic Materials, Elsevier Science, 2001.
[27] M. Kruk, M. Jaroniec, A. Sayari, Application of large pore MCM-41 molecular sieves to improve pore size analysis using nitrogen adsorption measurements, Langmuir 13 (1997) 6267–6273.
[28] M. Fernández, N. Bellotti, Silica-based bioactive solids obtained from modified diatomaceous earth to be used as antimicrobial filler material, Mater. Lett. 194 (2017) 130–134.
[29] W.D. Breck, Zeolite Molecular Sieves, Wiley, New York, 1974.
[30] L. Bortolatto, R. Boca Santa, J. Moreira, D. Machado, M. Martins, M. Fiori, N. Kuhnen, H. Riella, Synthesis and characterization of Y zeolites from alternative silicon and aluminium sources, Microporous Mesoporous Mater. 248 (2017) 214–221.
[31] G. Mille, J.L. Meyer, J. Chouteau, Δ-2 thiazoline et alkyl-2 Δ-2 thiazolines: etude vibrationnelle infrarouge et Raman.conformation, J. Mol. Struct. 50 (1978) 247–257.
[32] S. Lowell, J. Shields, M. Thomas, M. Thommes, Characterization of Porous Solids and Powders: Surface Area, Pore Size and Density, Springer Science+Business Media, LLC, The Netherlands, 2004.
[33] R. Yang, Adsorbents: Fundamentals and Applications, Wiley, New York, 2003.
[34] Z. Li, Use of surfactant-modified zeolite as fertilizer carriers to control nitrate release, Microporous Mesoporous Mater. 61 (2003) 181–188.
[35] W. Paulus, Compounds with activated halogen groups, in: Microbicides for the Protection of Materials, Springer, Dordrecht, 1993.